# Yield design based numerical analysis of three-dimensional reinforced concrete structures

Hugues Vincent, Mathieu Arquier, Jeremy Bleyer, Patrick de Buhan

4th International Conference on Mechanical Models in Structural Engineering
CMMoST 2017
29 nov-01 dec 2017 Madrid SPAIN

# Yield design based numerical analysis of three-dimensional reinforced concrete structures

**H. Vincent [1,2], M. Arquier[1], J. Bleyer[2], P. de Buhan[2]**

[1]*Strains. France. 23 Avenue d'Italie 75013, Paris, France*
[2]*Laboratoire Navier, UMR 8205, Ecole des Ponts ParisTech, IFSTTAR, CNRS, UPE, Champs-sur-Marne, France*

**ABSTRACT**

The purpose of this contribution is to present some new recent developments regarding the evaluation of the ultimate bearing capacity of massive reinforced concrete structures which cannot be modelled as 1D (beams) or 2D (plates) structural members. The approach is based on the implementation of the lower bound static approach of yield design through a discretization of the three-dimensional structure into tetrahedral finite elements, on the one hand, the formulation of the corresponding optimization problem in the context of Semidefinite Programming (SDP) techniques, on the other hand. Another key feature of the method lies in the treatment of the concrete embedded reinforcing bars not as individual elements, but by resorting to an extension of the homogenization approach. The whole procedure is first validated on a rather simple illustrative problem, then applied to the design of a bridge pier cap taken as an example of more complex and realistic structure.

*Keywords: reinforced concrete structures, yield design, semidefinite programming, homogenization*

## 1. INTRODUCTION

The yield design [1] or limit analysis [2] approach provides a suitable theoretical as well as computational framework for the Ultimate Limit State Design of reinforced concrete structures. In the situation when the structure is made of an assemblage of 1D (beams or arches) or 2D (plates or shells) structural members, its ultimate bearing capacity may be evaluated from the previous determination of interaction yield criteria involving generalized stresses such as axial-membrane forces and bending moments. This method, which proves particularly attractive from an engineering point of view, has been quite recently used for spatial frame structures [3] and reinforced concrete plates [4] in combination with efficient convex optimization procedures.

On the other hand, assessing the ultimate load bearing capacity of constructions incorporating massive three-dimensional reinforced concrete components, which can no more be modelled as beams or plates, requires a specific analysis, such as the widely acknowledged "strut-and-tie" model which, in some way, can be related to the lower bound static approach of yield design. With a special attention to evaluating the ultimate shear capacity of reinforced concrete deep beams, both the lower and upper bound methods of yield design have been implemented in the context of a finite element formulation with the help of linear programming techniques [5]. In this study, reinforced concrete was described according to a "mixed modelling" approach, in which plain concrete was modelled as a two-dimensional

continuous medium under plane stress, while the reinforcement bars were treated as one dimensional flexible beams embedded in the concrete material.

The generalization to the more realistic situation of linear reinforcing inclusions placed into three-dimensional concrete bodies is posing a somewhat serious challenge as regards the possibility of treating such a case in a 1D-3D mixed modelling approach. Some attempts to circumvent this problem have already been proposed either in the context of the finite element formulation [6] or making use of an implicit homogenization method [7] or multiphase model [8].

The present contribution is devoted to applying the previously mentioned multiphase model, initially developed for reinforced soils, to the yield design of three-dimensional reinforced concrete structures. It is based on the combination of the following elements.

- Formulation of the plain concrete three-dimensional strength properties by means of a tension cut-off Mohr-Coulomb condition, characterized by the uniaxial tensile and compressive strengths of the concrete, along with its friction angle.
- Modelling the strength of each individual reinforcement with its surrounding concrete volume as an anisotropic continuum accounting for the axial strength of the reinforcing inclusion.
- Finite element formulation of the lower bound static approach of yield design based on a discretization of the structure into tetrahedral elements with a piecewise linear variation of the stresses.
- The final optimization procedure is carried out by means of Semidefinite Programming (SDP).

The whole design procedure will be illustrated on the typical example of evaluating the ultimate bearing capacity of a reinforced concrete bridge pier cap subjected to concentrated vertical loads.

## 2. MODELLING STRENGTH PROPERTIES OF PLAIN AND REINFORCED CONCRETE

### 2.1. Plain concrete and reinforcing bars

Following the approach of [2] and [5] or quite recently [4], the unreinforced or plain concrete will be modelled as a 3D homogeneous continuous medium, the strength properties of which will be described by means of a *tension cut-off Mohr-Coulomb* yield condition which may be formulated as:

$$F^c(\underline{\underline{\sigma}}) = \sup\left\{K_p\sigma_M - \sigma_m - f_c; \sigma_M - f_t\right\} \leq 0 \tag{1}$$

In the above condition, $\sigma_M$ and $\sigma_m$ are the major and minor principal stresses, respectively (tensile stresses are counted positive throughout the text), $f_t$ and $f_c$ denote the uniaxial tensile and compressive resistances and $K_p=(1+\sin\varphi)/(1-\sin\varphi)$ where $\varphi$ is the internal friction angle which is usually taken equal to 37° ($K_p\approx4$). This criterion is thus defined by three strength parameters. It may be represented by means of an intrinsic curve in the Mohr-plane by as shown in Fig. 1, where the three material parameters defining the strength condition (1) are clearly apparent.

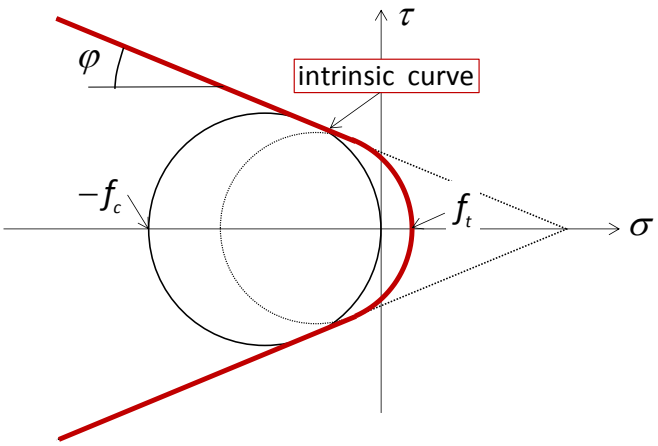


**Figure 1.** *Geometrical representation of the tension-cutoff Mohr-Coulomb criterion in the Mohr-plane*

The concrete material is reinforced by one dimensional steel bars or rods, the strength condition of which may be expressed in terms of axial force *N* only, since their resistance to shear force *V* and bending moment *M* is neglected:

$$-kN_0 \le N \le N_0,\ V = M = 0 \tag{2}$$

In the above condition, $N_0$ denotes the tensile resistance of each individual reinforcing bar, while *k* is a non-dimensional parameter, ranging from 0 to 1, which accounts for a reduced resistance under compression, due to buckling for instance.

### 2.2. Reinforced concrete: a homogenized strength condition

Some significant zones of the reinforced concrete structure (such as deep beams: see for instance [2]) may be reinforced by such uniformly distributed bars (case of stirrups or open frames). Provided that the spacing between two neighbouring reinforcements is sufficiently small as compared with the size of the reinforced zone, the latter may be replaced by a zone where the homogenized constituent material obeys a *macroscopic strength condition* (see [9] for composite materials, or [10] for reinforced soils and [5] for reinforced concrete).

This macroscopic strength condition, which can be derived from using the *yield design homogenization method* [11], may be expressed as follows:

$$F^{rc}(\underline{\underline{\sigma}}) \le 0 \Leftrightarrow \begin{cases} \underline{\underline{\sigma}} = \underline{\underline{\sigma}}^c + \sigma^r \underline{e}_1 \otimes \underline{e}_1 \\ \text{with} \quad F^c(\underline{\underline{\sigma}}^c) \le 0 \ \text{ and } \ -k\sigma_0 \le \sigma^r \le \sigma_0 \end{cases} \tag{3}$$

where $\underline{e}_1$ is the unit vector parallel to the reinforcing bar, and $\sigma_0$ is defined as the tensile resistance of the bars *per unit transverse area*:

$$\sigma_0 = \frac{N_0}{s^2} \tag{4}$$

which may also be expressed as:

$$\sigma_0 = \frac{A^s f_y^s}{s^2} = \eta f_y^s \tag{5}$$

where $f_y^s$ denotes the uniaxial strength of the bar constituent material (steel) and $A^s$ the bar cross-sectional area, so that $\eta$ represents the *reinforcement volume fraction* (see Fig. 2(*a*) where $s^2 = A^s + A^c$).

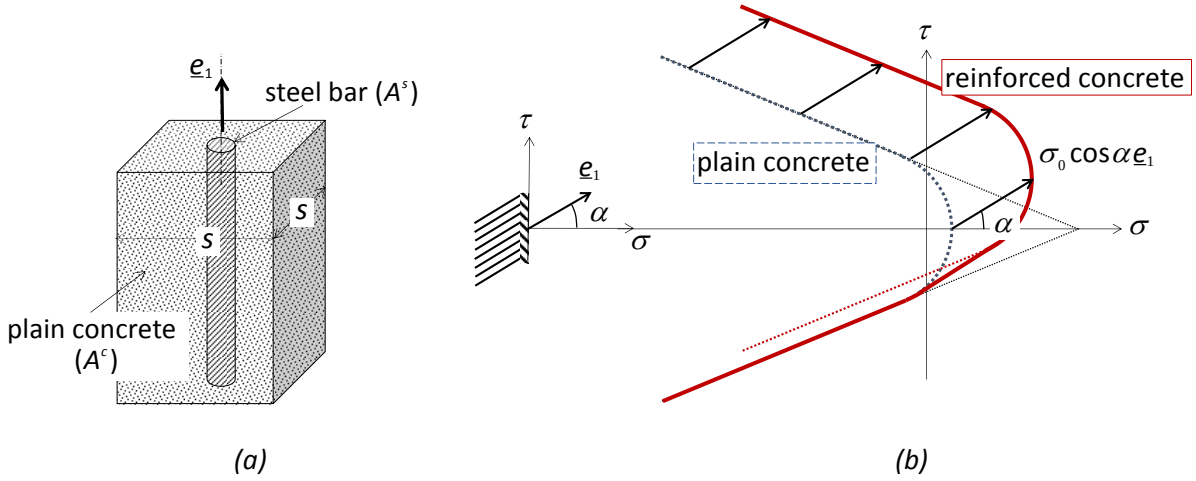


**Figure 2.** *(a) Representative volume of reinforced concrete; (b) macroscopic strength condition relative to an oriented facet (case k=0)*

It is to be noted that the validity of the above macroscopic strength criterion (3) is subject to the verification of two important conditions (see [11] for more details).

- The reinforcing bars are perfectly bonded to the surrounding concrete material, which means for instance that no slippage occurs at the bar/concrete interface.
- The reinforcement volume fraction remains sufficiently small ($\eta$<<1), whereas the resistance of the reinforcing material is much higher than that of the concrete material and notably its tensile strength ($f_y^s >> f_t$).

Figure 2(*b*) illustrates the macroscopic strength condition (3) expressed on an oriented facet of the homogenized reinforced concrete in the particular case when *k*=0 (no compressive resistance of the reinforcements). The corresponding strength domain in the $(\sigma,\tau)$-plane can be drawn simply as the convex envelope of the plain concrete intrinsic failure curve and of the curve derived from that one through a translation of vector $\sigma_0 \cos\alpha \underline{e}_1$. Such a geometric representation thus gives a clear evidence of the *strength anisotropy* of the homogenized reinforced concrete in exactly the same way as for fibre composite materials.

It should be pointed out that, without any reference to the limit analysis or yield design homogenization theory, some authors [7] did make use of a strength criterion quite similar to (3), that is based on an intuitive additive decomposition of the total stress in reinforced concrete zones into stress components relating to the plain concrete and the reinforcements, each one complying with independently specified strength conditions.

### 2.3. The "mixed modelling" approach to reinforced concrete structures: a serious limitation

Referring to the frequently encountered situation where only a small number of differently oriented reinforcements are incorporated in the concrete structure (case of longitudinal reinforcements in deep beams for instance), the above mentioned homogenization method is no more applicable and the so-called *"mixed modelling" approach* should be advocated. According to this approach, the reinforcements are treated as 1D structural elements with a strength condition defined by (2)

embedded in the concrete material modelled as a 3D continuum, the strength of which is specified by (1).

Unfortunately, this 1D-3D mixed modelling approach comes against a serious limitation concerning the establishment of equilibrium equations for such a composite system. Indeed, the equilibrium equation at any point of the reinforcing bar may be written as:

$$\frac{\mathrm{d}N(x_1)}{\mathrm{d}x_1} + p(x_1) = 0 \tag{6}$$

where $p$ represents the density of axial force exerted by the surrounding concrete material onto the reinforcing bar (Fig. 3(*a*)).

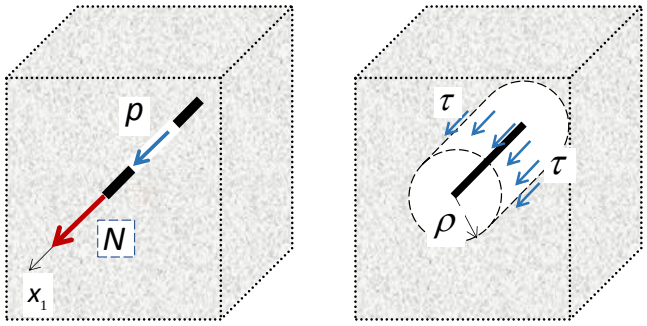


(*a*) (*b*)

**Figure 3.** Interaction forces between concrete and reinforcement in the context of 1D-3D mixed modelling

Now, the impossibility of connecting such a 1D distribution $p$ of interaction forces with the three-dimensional stress fields prevailing in the concrete material may be illustrated from the following simple reasoning. Considering a circular cylindrical "control surface" of radius $\rho$ with its axis placed along the reinforcement, as shown in Fig. 3(*b*), the interaction force density $p$ may be obtained from applying along this surface a longitudinal shear stress $\tau$, the average value of which along the circle drawn on this surface at point $x_1$, could be expressed as:

$$\langle \tau \rangle (x_1) = \frac{p(x_1)}{2\pi\rho} \tag{7}$$

According to the latter equation, the shear stress which should be developed in the concrete along the control surface for applying a given value of interaction force density $p$ increases to infinity as the radius $\rho$ tends to zero, so that the stress field in the concrete material would tend to infinity along the reinforcement axis. Such a singularity could possibly be taken into account in the context of a linear elastic behavior of the concrete, but definitely not as soon as yielding and failure of the latter is concerned, since in this case the yield strength condition (1) of the concrete would be systematically violated when approaching the 1D reinforcing bar.

### 2.4. An extended homogenization-based model

Of course, the only fully mechanically consistent and rigorous way of circumventing the above limitation, would be to model each reinforcing bar as a three-dimensional volume body. But, on account of the small diameter of such bars along with the sharp contrast between the reinforcing steel and the surrounding concrete in terms of strength properties, this would undoubtedly imply prohibitive computational costs, due for instance to the highly refined discretization required when employing finite element techniques.

An alternative approach for the finite element modelling of 1D steel inclusions in 3D concrete volumes has been recently proposed by [6]. Likewise, in a more explicit reference to the homogenization procedure, three dimensional fem elastoplastic analyses on reinforced concrete structural elements have been performed by [8]. Their approach, which will be adopted in this contribution, may be described as follows.

Considering one individual 1D-inclusion embedded in a 3D-concrete block, a cylindrical volume of concrete with the inclusion placed along its axis is defined, as shown in Fig. 4(a). The intuitive idea is to replace the composite cylindrical volume, thus obtained, by a homogenized cylinder, at any point of which the strength condition is defined by Eqs. (3) and (4), where *s* represents the side of the squared cross-section of the cylindrical volume.

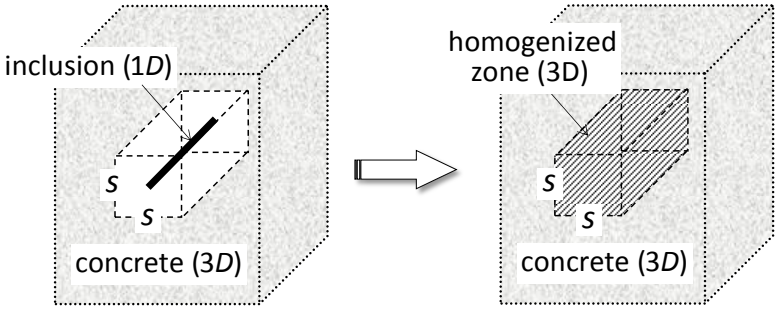


**Figure 4.** *Construction of a homogenized reinforced zone around an individual inclusion*

The advantage of such a modelling procedure, is that the characteristic size of the homogenized zone (namely *s*) is significantly larger than the inclusion's diameter, thus allowing for example a much easier finite element discretization of the reinforced concrete structure as a 3D-3D composite, since a refinement of the mesh around the inclusion is no more required for obtaining accurate and reliable predictions. Of course, the choice of *s* being arbitrary, it will be necessary to make sure that the results of the computations performed on the basis of this model, remain rather insensitive to the value of *s*.

## 3. NUMERICAL IMPLEMENTATION OF THE LOWER BOUND STATIC APPROACH

### 3.1. Statement of the yield design problem

Assuming that the reinforced concrete structure under consideration is subject to *one single loading parameter Q*, the *ultimate* or *failure load value* $Q^+$ is defined, in the context of the yield design theory, as the maximum value of *Q* for which one can exhibit any stress field $\underline{\underline{\sigma}}$:

- ✓ *statically admissible* (S.A.) with *Q*, *i.e.* verifying the equilibrium equation at any point of the structure:

$$\mathrm{div}\,\underline{\underline{\sigma}}(\underline{x}) + \rho\underline{F}(\underline{x}) = 0,\ \forall \underline{x} \in V \tag{8}$$

where $\rho\underline{F}$ denotes the body force volume density (material specific weight for example), along with the continuity of the stress-vector across possible stress jump surfaces $\Sigma$:

$$\left[\underline{\underline{\sigma}}(\underline{x})\right].\underline{n}(\underline{x}) = 0, \quad \forall \underline{x} \in \Sigma \tag{9}$$

as well as the stress boundary conditions associated with the loading *Q*;

- ✓ and complying with the *strength conditions* assigned to the plain concrete and reinforced concrete zones of the structure, respectively*:*

$$F^c(\underline{\underline{\sigma}}(\underline{x}))\leq 0\ \forall \underline{x}\in V^c \ \text{ and } \ F^{rc}(\underline{\underline{\sigma}}(\underline{x}))\leq 0\ \forall \underline{x}\in V^{rc},\ \ V=V^c\cap V^{rc} \tag{10}$$

where $V^c$ (respectively $V^{rc}$) represents the part of the structure occupied by the plain concrete (resp. by the homogenized reinforced concrete).

### 3.2. 3D finite element discretization

Applying the *lower bound static approach* consists in considering S.A. stress fields depending either on a small number of parameters in an analytical approach, or on a large but finite number of stress variables in a numerical approach, such as the finite element method. According to the latter, the geometrical domain $V$ occupied by the three-dimensional structure is discretized into $N_e$ tetrahedral finite element $V^e$, such as the one depicted in Fig. 5(*a*), with a *linear variation* of the stress field inside each element so that the stress at any point inside such an element may be classically written as:

$$\forall \underline{x}\in V^e,\ \underline{\underline{\sigma}}(\underline{x})=\sum_{k=1}^{4} N^k(\underline{x})\underline{\underline{\sigma}}^k \tag{11}$$

where $N^k$ are four linear interpolation functions and $\underline{\underline{\sigma}}^k$ is the value of the stress tensor at the node n°$k$ of the element. It is to be noted that there are as many stress tensors attached to any geometrical node of the mesh as there are tetrahedral elements sharing this node as an apex.

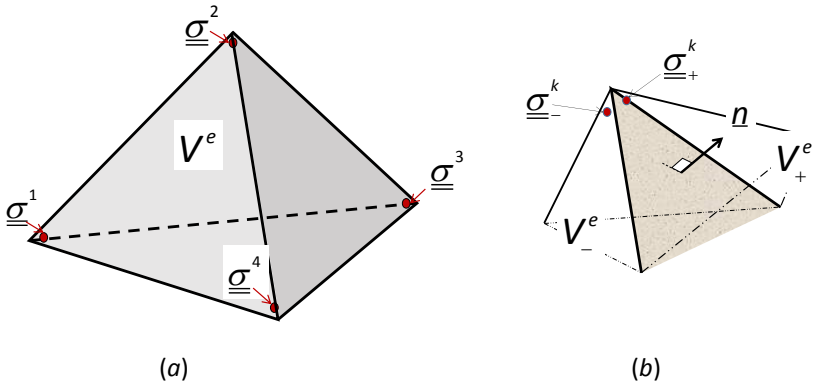


(*a*) (*b*)

**Figure 5.** *Four nodded tetrahedral finite element used in the discretization of the reinforced concrete structure*

Furthermore, one may come across two situations.

- ✓ The considered element is located in the *unreinforced plain concrete* zone $V^c$ of the structure, so that the stress state at any node of this element is defined by one single tensor which should comply with the strength condition (1).
- ✓ The element is located in the *homogenized reinforced concrete* zone $V^{rc}$, and, as suggested by the corresponding homogenized strength condition (3), the stress state is defined by a stress tensor and an additional scalar stress variable which must satisfy separate independent strength conditions.

It follows that a total of, either 4x6=24 or 4x7=28 stress variables are attached to each element $V^e$ of the mesh.

### 3.3. Formulation of equilibrium conditions as linear constraints on the stress variables

On account of (11), the equilibrium equation (8) inside each element may be rewritten as:

$$\forall \underline{x} \in V^e,\ \mathrm{div}\underline{\underline{\sigma}}(\underline{x}) = \sum_{k=1}^{4} \underline{\mathrm{grad}N^k}.\underline{\underline{\sigma}}^k = -\rho \underline{F} \tag{12}$$

where it is assumed that the body force density is constant over the element. Since the gradient of each interpolation function is constant, Eq. (11) represents a *linear constraint* on the nodal stress variables $\underline{\underline{\sigma}}^k$ of each element. It is worth noting that the linear equilibrium condition (11) involves the *total* stress in the homogenized reinforced concrete and not the "partial" stresses $\underline{\underline{\sigma}}^c$ and $\sigma^r$ which appear in the definition (3) of the reinforced concrete strength condition.

Likewise, Eq. (8) expresses the continuity of the (total) stress vector across any triangular facet common to two adjacent elements (see Fig. 5(*b*)). It also leads to *linear constraints* of the form:

$$(\underline{\underline{\sigma}}_+^k - \underline{\underline{\sigma}}_-^k).\underline{n} = 0 \tag{13}$$

where $\underline{n}$ is the unit normal to the triangular facet connecting two such adjacent elements $V_+^e$ and $V_-^e$. Owing to the linear variation of the stress fields, checking the jump condition (13) at the nodal points is sufficient to make sure that it is verified at any point of the discontinuity triangular facet.

It follows that all the conditions that a discretized stress field must satisfy for being statically admissible with a load value *Q* may be formulated in a generic matrix form as:

$$\underline{\underline{\sigma}}^{\mathrm{fem}} \text{ S.A. with } Q \Leftrightarrow \begin{cases} Q = {}^T\{A\}\{\Sigma\} \\ \text{with } [B]\{\Sigma\} = \{C\} \end{cases} \tag{14}$$

where $\{\Sigma\}$ is a column-vector which collects all the nodal stress variables associated with the mesh discretization of the structure, that is the total stresses in the plain concrete zones and the partial stresses in the homogenized reinforced parts.

Consequently, the finite element implementation of the lower bound static approach of yield design reduces to the following maximisation problem:

$$Q^+ \geq Q^{lb} = \underset{\{\Sigma\}}{\mathrm{Max}}\ Q = {}^T\{A\}\{\Sigma\} \text{ subject to } \begin{cases} [B]\{\Sigma\} = \{C\} & \text{equilibrium} \\ F(\{\Sigma\}) \leq 0 & \text{strength criteria} \end{cases} \tag{15}$$

where $F(\{\Sigma\}) \leq 0$ represents the conditions expressing the different *strength criteria* to be satisfied. Again, due to the linear variations (11) of the considered stress fields and to the *convexity* of the strength conditions, the latter have only to be verified at the nodal stress points.

### 3.4. Formulation as a SDP problem

Unlike the equilibrium conditions which involve the total stresses only, the strength criteria in the homogenized reinforced zones concern the partial stresses as shown by (3). While the condition relating to the reinforcement writes in the form of a simple *linear* constraint ($-k\sigma_0 \leq \sigma^r \leq \sigma_0$), the strength

condition of the plain concrete defined by (1) involves the maximal and minimal principal stress components. The latter thus needs a specific treatment so that the optimization problem (15) may be treated as a *Semidefinite programming* (SDP) optimization problem [12] as briefly explained below.

*Semidefinite Programming* allows to formulate optimization problems in terms of constraints on eigenvalues of symmetric matrices. It therefore provides a suitable framework for the tension cut-off Mohr-Coulomb criterion (1) which involves the maximal and minimal principal stress components (eigenvalues). Thus, the three-dimensional Mohr-Coulomb criterion can be enforced by applying the two *linear matrix inequalities* (LMI):

$$t_M \underline{\underline{1}} - \underline{\underline{\sigma}} \succeq 0 \quad \text{and} \quad t_m \underline{\underline{1}} - \underline{\underline{\sigma}} \preceq 0 \,^{1} \tag{16}$$

in conjunction with the equality constraint:

$$K_p t_M - t_m - f_c = 0 \tag{17}$$

where $t_M$ and $t_m$ are auxiliary variables. Eliminating $t_M$ from Eq. (17) yields:

$$\underline{\underline{\sigma}} - K_p^{-1} t_m \underline{\underline{1}} \preceq K_p^{-1} f_c \underline{\underline{1}} \quad \text{and} \quad t_m \underline{\underline{1}} - \underline{\underline{\sigma}} \preceq 0 \tag{18}$$

The second inequality of (18) can be expressed as:

$$t_m \underline{\underline{1}} - \underline{\underline{\sigma}} + \underline{\underline{X}} = 0 \ \text{ and } \ \underline{\underline{X}} \succeq 0 \tag{19}$$

where $\underline{\underline{X}}$ is an auxiliary symmetric matrix included in the convex cone of positive semidefinite matrices. It allows the stress variable to be eliminated using the relationship:

$$\underline{\underline{\sigma}} = t_m \underline{\underline{1}} + \underline{\underline{X}} \tag{20}$$

so that the first inequality of (18) becomes:

$$\underline{\underline{X}} + (1 - K_p^{-1}) t_m \underline{\underline{1}} \preceq K_p^{-1} f_c \underline{\underline{1}} \tag{21}$$

Introducing $\underline{\underline{Y}}$ as a second auxiliary symmetric matrix variable, the three-dimensional Mohr-Coulomb strength criterion may finally be reformulated as:

$$\begin{aligned} &\underline{\underline{X}} + \underline{\underline{Y}} + (1 - K_p^{-1}) t_m \underline{\underline{1}} \ = \ K_p^{-1} f_c \underline{\underline{1}} \\ &\text{with} \ \ \underline{\underline{X}} \succeq 0 \ \text{ and } \ \underline{\underline{Y}} \succeq 0 \end{aligned} \tag{22}$$

which lends itself very easily to the numerical treatment by a SDP solver such as [13].

Similarly, the Rankine-type cut-off strength criterion which limits the tensile stresses in the plain concrete material:

$$\sigma_M - f_t \leq 0 \Leftrightarrow \underline{\underline{\sigma}} - f_t \underline{\underline{1}} \preceq 0 \tag{22}$$

may be recast into the following constraints:

$$\underline{\underline{\sigma}} + \underline{\underline{Z}} - f_t \underline{\underline{1}} = 0 \ \text{ and } \ \underline{\underline{Z}} \succeq 0 \tag{23}$$

where a third auxiliary symmetric matrix variable has been introduced.

[1] where $\underline{\underline{A}} \succeq 0 \Leftrightarrow \underline{x}.\underline{\underline{A}}.\underline{x} \geq 0 \ \forall \underline{x}$

## 4. A FIRST ILLUSTRATIVE TEST EXAMPLE

A specific computer code implementing the whole above described numerical procedure, has been devised for calculating *optimized lower bounds* to the ultimate loads of three dimensional reinforced concrete structures. A first illustrative application of this code is performed on the illustrative example of a beam of length $L$=4 m and rectangular cross-section ($H$=0.5 m, $b$=0.2 m), subject to a uniform surface loading $q$ applied onto the top of the beam (Fig. 6). The left end (X=0) of the beam is perfectly *clamped* (velocity vector equal to zero: $\underline{U}$=0), while the boundary conditions at the right end (X=$L$) are:

$$T_x = \sigma_{xx} = 0,\ U_y = U_z \tag{24}$$

which, within the framework of a 1D model of the beam, would correspond to a simple support free to mode horizontally (no axial force and bending moment are applied).

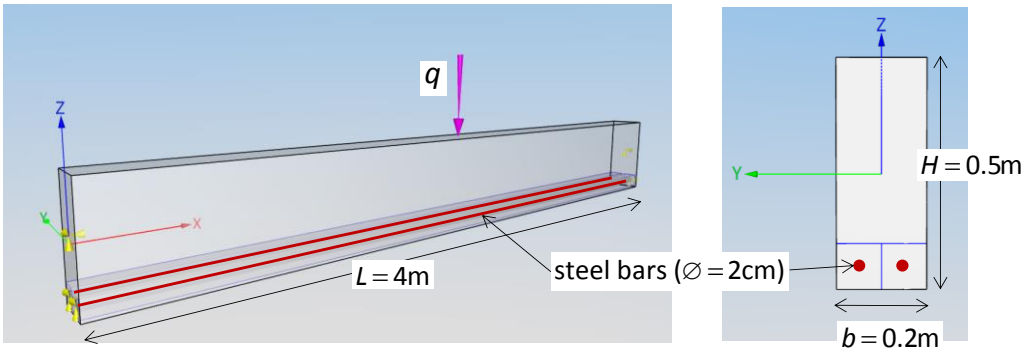


**Figure 6.** Reinforced concrete beam under uniform loading

The beam is made of a homogeneous concrete material, with the following uniaxial tensile and compressive strength characteristics:

$$f_t = 0.5 \text{ MPa} \quad \text{and} \quad f_c = 40 \text{ MPa} \tag{25}$$

keeping in mind that, referring to a tension cut-off Mohr-Coulomb condition, the value of the internal friction angle $\varphi$ is taken equal to 37°.

The beam is reinforced by two longitudinal rebars of diameter equal to 2cm, made of a steel with a uniaxial strength equal to $f_y^s$ =400 MPa. The bars are placed at the bottom part of the beam cross section as shown in Fig.5. According to the method described in 2.4, each bar with its surrounding volume of concrete material is replaced by a homogenized material obeying the macroscopic strength condition (3) with:

$$\sigma_0 = \frac{\pi \varnothing^2 f_y^s}{4 s^2} \tag{26}$$

where $s^2$ is the cross-section area of the homogenized volume, which is varied between $s^2=(b/2)^2=0.01$ m$^2$ (case of Fig. 6) and $s^2=0.005$ m$^2$.

The whole structure being discretized into less than 3 000 tetrahedral finite elements (2 656 for the case presented in Fig. 7), the SDP maximization procedure described earlier, is performed for four configurations associated with decreasing values of the homogenized area $s^2$. A longitudinal view of the

optimized stress field is represented for instance in Fig. 7 for $s^2$=0.01 m$^2$. The top figure shows the distribution of the *principal compressive stresses* prevailing in the plain concrete material, while the intermediate figure represents the *principal tensile stresses* mobilized in the (homogenized) reinforcement. Both distributions are superimposed in the bottom figure. Calculations were performed on a laptop computer with an INTEL CORE i7 – CPU @ 2.4 GHz in about 250 seconds (four minutes) depending on the case.

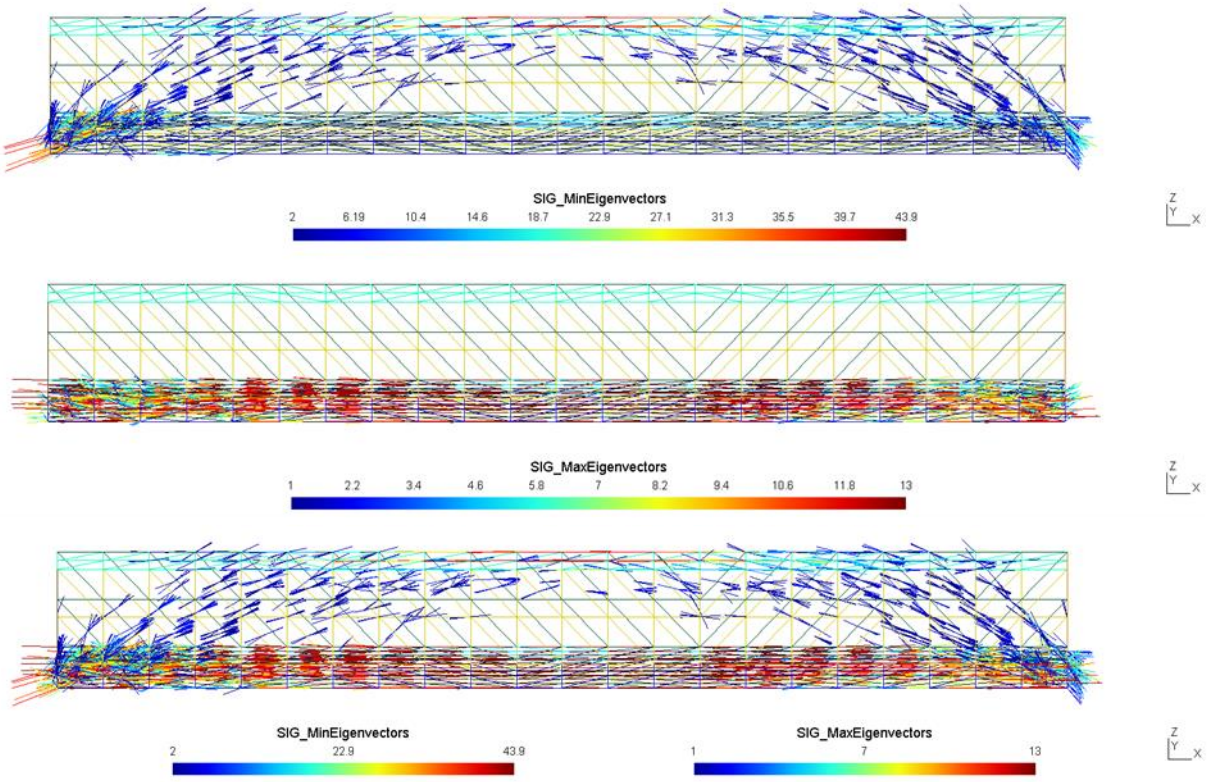


**Figure 7.** Longitudinal view of the optimized stress field in the concrete

The most important and relevant results obviously concern the obtained lower bound evaluation of the ultimate bearing capacity of the reinforced concrete beam. These are reported in Fig. 8 in the form of curves giving this evaluation for the un-reinforced and reinforced beam as a function of the homogenized area, the same mesh being used for the un-reinforced and reinforced cases.

Two comments are worth being made from observing this graph:

- ✓ Even if it should be recalled that the obtained results are *lower bound estimates* for the exact ultimate bearing capacity of the beam, the strengthening effect due to the presence of the bars in the concrete beam is striking, since the evaluation of the ultimate failure load, equal to $q$=40 kPa for the plain concrete beam is increased to more than $q$=300 kPa when the reinforcement by two longitudinal bars is taken into account.

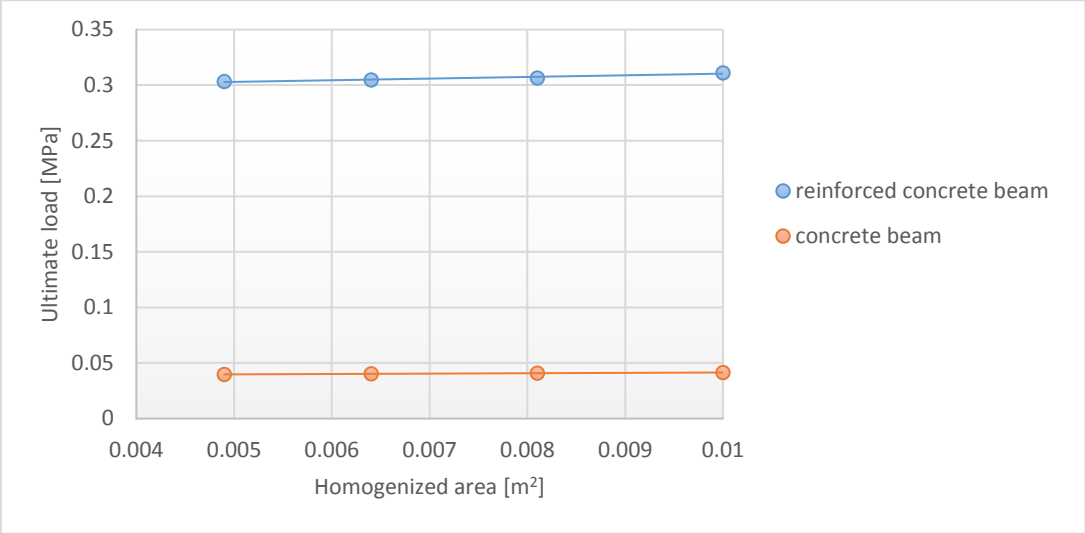


**Figure 8.** Lower bound evaluation of the beam ultimate bearing capacity as a function of the homogenization area

- ✓ Furthermore, the validity of the proposed homogenization method for treating the case of a reinforcement by few individual inclusions, is clearly demonstrated by the upper curve. Indeed, the latter is nearly horizontal (very slight increase), which means that the numerical lower bound estimate is almost insensitive to the size of the homogenised area. This underlines the decisive advantage of the proposed homogenization method over a direct approach where the inclusion should be finely discretized, thus leading to an oversized numerical problem.

## 5. A PRACTICAL CASE STUDY: FAILURE DESIGN OF A BRIDGE PIER CAP

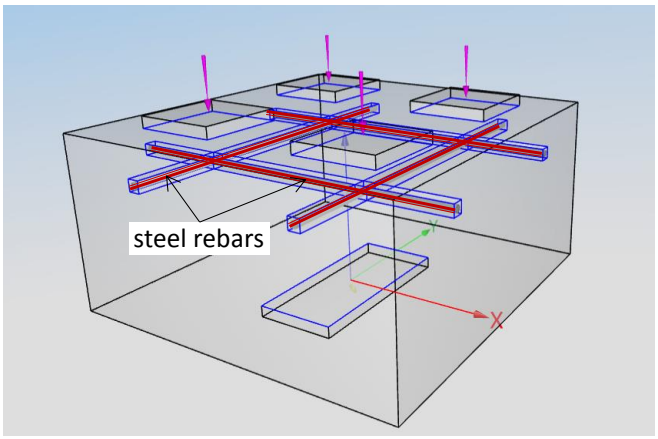


**Figure 9.** Reinforced concrete pier cap subject to bridge deck loading

In order to assess the performance of the yield design numerical tool in situations where truly massive three dimensional structures are involved, the following representative design case is now examined: a 3x3x1.5 $m^3$ parallelepipedic concrete block is considered as a simplified model of bridge pier cap. The finite element lower bound static approach is performed on this structure subject to four vertical loads representing the action of the overlying bridge deck, as shown in Fig. 9. These loadings are applied in the form of a uniform pressure applied on top of small rigid square pads of 0.7x 0.7 $m^2$. The interaction

with the underlying bridge pier is modelled by imposing a rigid connection on a 1.5x0.7 $m^2$ rectangular area placed at the centre of the bottom surface.

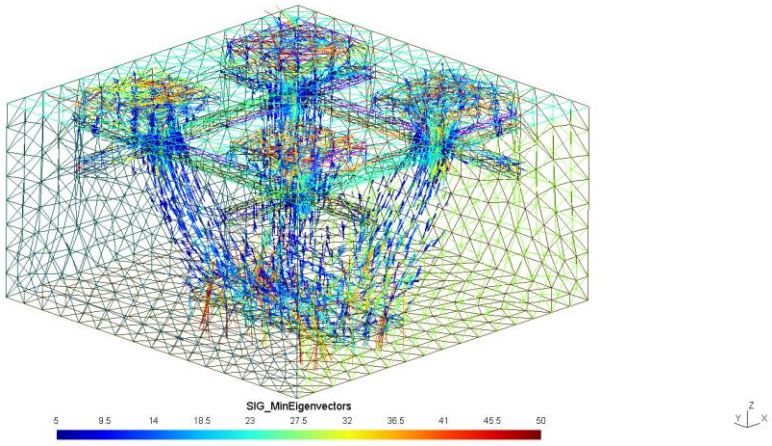


**Figure 10.** Perspective view of the optimized stress field in the concrete

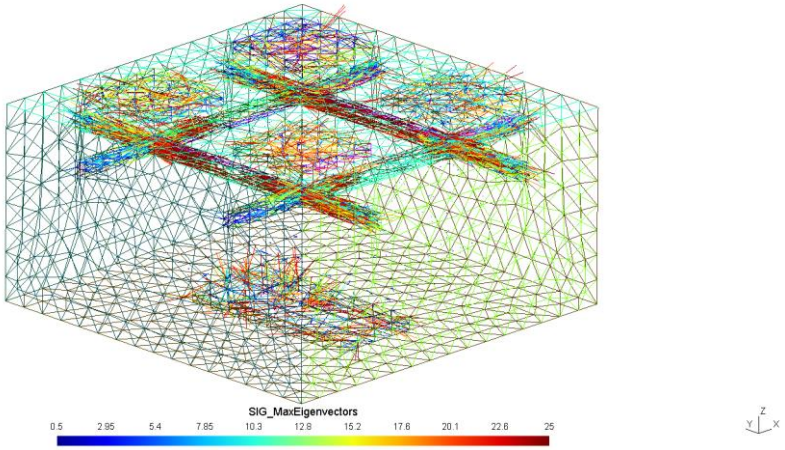


**Figure 11.** Optimized stress field in the homogenized zone

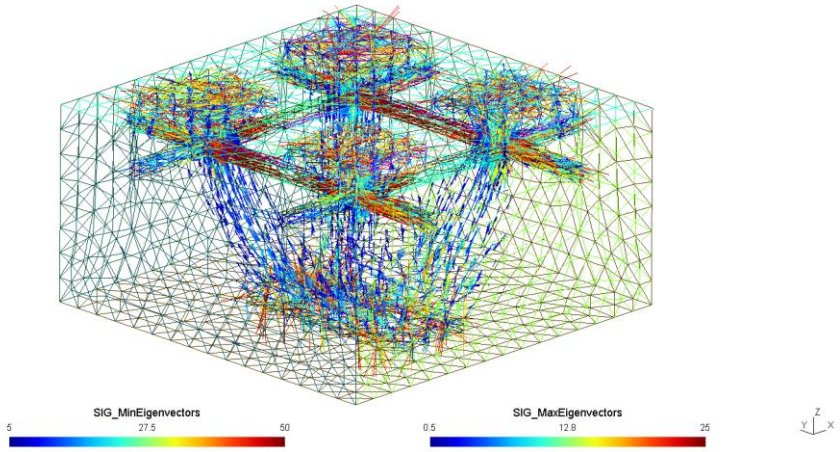


**Figure 12.** View of the optimized stress field in the whole pier cap

The concrete block is made of a homogeneous plain concrete material, with $f_c = 40$ MPa and $f_t = 0.5$ MPa. It is strengthened by four steel rebars of diameter equal to 3cm, placed just below the

loading pads as shown in Fig. 9, with a uniaxial strength equal to $f_y^s$ =400 MPa. According to the above described procedure procedure, each of the four rebars is replaced by an homogenized volume of square cross section equal to $s^2$=0.01 m$^2$.

The whole structure being discretized into 33 632 tetrahedral finite elements, an optimal lower bound estimate for its ultimate load bearing capacity has been obtained using the SDP maximization procedure. Fig. 10 represents the distribution of the *principal compressive stresses* prevailing in the plain concrete material, while Fig. 11 the *principal tensile stresses* mobilized in the (homogenized) reinforcement. Both distributions have been superimposed in Fig. 12. Calculations were performed on the same laptop computer in approximately 4 000 seconds (one hour).

The thus obtained lower bound estimate for the ultimate bearing capacity of the reinforced concrete structure is equal to 4.56 MPa on each of the four loading pads. By way of comparison, the lower bound evaluation of the ultimate bearing capacity of the same *non-reinforced* concrete structure is equal to 3.18 MPa. This means that the presence of the reinforcements increases the global resistance of the pier cap by as much as 44 %.

The proposed model of three-dimensional reinforced concrete structures advocated in this contribution, as well as the feasibility of the related numerical approach in the context of the finite element method, have thus been successfully tested here on a more complex 3D case. Fig. 12 in particular gives a clear intuition of the optimized stress field equilibrating the applied loading, exhibiting compressive stresses (*struts*) in the concrete material and tensile stresses in the homogenized reinforced zones (*ties*).

## 6. CONCLUSION

A specifically dedicated finite element computer code has been set up aimed at producing rigorous lower bound (*i.e.* conservative) estimates for the ultimate load bearing capacity of three-dimensional reinforced concrete structures in the context of the yield design approach. It relies upon two recent decisive breakthroughs: the numerical formulation of the corresponding optimization problem using Semidefinite Programming, on the one hand, the adoption of a homogenization-inspired model for describing the mechanical behaviour of individual reinforcing inclusions embedded in a surrounding three-dimensional concrete matrix, on the other hand. The procedure may be further extended on two important points.

- The development of the same kind of numerical method and related computer tool in the framework of the yield design kinematic approach, which will provide upper bound estimates. Comparing the latter with the already determined lower bound estimates, will considerably help improve the accuracy and reliability of the design procedure.
- The adoption of a multiphase model, which may be perceived as an extension of the homogenization method [11], making it possible to take a specific interaction failure condition between the reinforcements and the concrete material, into account.

**REFERENCES**

[1] Salençon J. (2013) Yield Design, ISTE Ltd, Wiley, London.

[2] Chen W.F. (1982) Plasticity in reinforced concrete, McGraw-Hill, New-York.

[3] Bleyer J., de Buhan P. (2013). Yield surface approximation for lower and upper bound yield design of 3D composite frame structures, *Computers and Structures*, 129, pp. 86-98.

[4] Bleyer J., Pham D.T., de Buhan P. (2015). Failure design of high-rise concrete panels under fire loading, *Engineering and Computational Mechanics*, Volume 168 Issue EM4, pp. 178-185.

[5] Averbuch D., de Buhan P. (1999). Shear Design of Reinforced Concrete Deep Beams: A Numerical Approach, *Jl. of Structural Engineering*, Volume 125, N°3, pp. 309-318.

[6] Llau A., Jason L., Dufour, F., Baroth J. (2016). Finite element modelling of 1D steel components in reinforced and pre-stressed concrete structures, *Engineering Structures*, 127, pp. 769-783.

[7] Nielsen M.P., Hoang L.C. (2010). Limit Analysis and Concrete Plasticity, CRC Press, Taylor & Francis.

[8] Figueiredo M.P., Maghous S., Filho A.C. (2013). Three-dimensional finite element analysis of reinforced concrete structural elements regarded as elastoplastic multiphase media, *Materials and Structures*, 46, pp. 383-404.

[9] de Buhan P., Taliercio A. (1991). A homogenization approach to the yield strength of composite materials, *European Journal of Mechanics*, A/Solids, 10, n°2, pp. 129-150.

[10] Michalowski P.V., Zhao A. (1996). Failure of fiber-reinforced granular soils, *Jl. Geotech. Eng.,* ASCE, 122(3), pp. 226-234.

[11] de Buhan P., Bleyer J., Hassen G. (2017). Elastic, Plastic and Yield Design of Reinforced Structures, ISTE Ltd, Wiley, London.

[12] Martin C.M., Makrodimopoulos A. (2008). Finite–Element Limit Analysis of Mohr-Coulomb Materials in 3D Using Semidefinite Programming, *Jl. Eng Mech.,* ASCE, Vol. 134, N°4, pp. 339-347.

[13] The Mosek optimization software: available from http://www.mosek.com